

# Probabilistic Modeling of Knee Muscle Moment Arms: Effects of Methods, Origin–Insertion, and Kinematic Variability

SAIKAT PAL,<sup>1</sup> JOSEPH E. LANGENDERFER,<sup>1</sup> JOSHUA Q. STOWE,<sup>1</sup> PETER J. LAZ,<sup>1</sup> ANTHONY J. PETRELLA,<sup>2</sup> and PAUL J. RULLKOETTER<sup>1</sup>

<sup>1</sup>Computational Biomechanics Lab, Department of Mechanical & Materials Engineering, University of Denver, 2390 S. York, Denver, CO 80208, USA; and <sup>2</sup>DePuy, a Johnson & Johnson Company, Warsaw, IN, USA

(Received 26 December 2006; accepted 21 May 2007; published online 2 June 2007)

**Abstract**—In musculoskeletal modeling, reliable estimates of muscle moment arms are an important step in accurately predicting muscle forces and joint moments. The degree of agreement between the two common methods of calculating moment arms—tendon excursion (TE) and geometric origin–insertion, is currently unknown for the muscles crossing the knee joint. Further, measured moment arm data are subject to variability in estimation of attachment sites as points from irregular surfaces on the bones, and due to differences in joint kinematics observed *in vivo*. Thus, the objectives of the present study were to compare moment arms of major muscles crossing the knee joint obtained from TE and geometric methods using a finite element-based lower extremity model, and to quantify the effects of potential muscle origin–insertion and tibiofemoral kinematic variability on the predicted moment arms using probabilistic methods. A semiconstrained, fixed bearing, posterior cruciate-retaining total knee arthroplasty was included due to available *in vivo* kinematic data. In this study, muscle origin and insertion locations and kinematic variables were represented as normal distributions with standard deviations of 5 mm for origin–insertion locations and up to 1.6 mm and 3.0° for the kinematic parameters. Agreement between the deterministic moment arm calculations from the two methods was excellent for the flexors, while differences in trends and magnitudes were observed for the extensor muscles. Model-predicted deterministic moment arms from both methods agreed reasonably with the experimental values from available literature. The uncertainty in input parameters resulted in substantial variability in predicted moment arms, with the size of 1–99% confidence interval being up to 41.3 and 35.8 mm for the TE and geometric methods, respectively. The sizeable range of moment arm predictions and associated excursions has the potential to affect a muscle's operating range on the force–length curve, thus affecting joint moments. In this study, moment arm predictions were more dependent on muscle origin–insertion locations than the kinematic variables. The important parameters from the TE method were the origin and

insertion locations in the sagittal plane, while the insertion location in the sagittal plane was the dominant parameter using the geometric method.

**Keywords**—Moment arm, Muscle excursion, Muscle path, Variability, Muscle origin, Muscle insertion, Finite element modeling, Probabilistic methods, Muscle attachment.

## INTRODUCTION

Reliable prediction of muscle moment arms is essential for the calculation of muscle forces and joint moments.<sup>27</sup> When model-predicted moment arms agree with measured *in vivo* or *in cadavera* data, the musculotendon excursion with respect to changes in joint angle is accurate, thus ensuring the musculoskeletal model reflects a physiological range of excursion. With physiologically correct excursion, muscle length-tension dependence can be incorporated to provide reliable predictions of muscle forces and joint moments.<sup>31</sup>

The two widely used methods of measuring moment arms are the tendon excursion (TE) method<sup>1,6</sup> and the geometric origin–insertion method.<sup>15,19,23,33</sup> Using the TE method, Buford *et al.* determined the flexion–extension moment arms of the major knee muscles from 15 cadaver specimens.<sup>6</sup> Arnold *et al.* developed an experimentally verified model of the lower extremity to predict musculotendon moment arms,<sup>2</sup> while Blemker and Delp created a finite element (FE) model to evaluate the effects of complex muscle architectures on fiber excursions.<sup>3</sup> Previous studies using the geometric method include moment arms derived from magnetic resonance (MR) imaging,<sup>25,35,39</sup> X-rays<sup>30</sup> or video fluoroscopy,<sup>20</sup> and about different axes of rotations: the instantaneous center of rotation,<sup>30</sup> the cruciate ligaments intersection point,<sup>12,18</sup> the tibiofemoral contact point<sup>15,20</sup> or the instantaneous screw axis (ISA).<sup>23</sup>

Address correspondence to Joseph E. Langenderfer, Computational Biomechanics Lab, Department of Mechanical & Materials Engineering, University of Denver, 2390 S. York, Denver, CO 80208, USA. Electronic mail: jlangend@du.edu

Although comparisons of moment arm estimates from TE and geometric methods were reported for the muscles of the shoulder<sup>17</sup> and ankle joints,<sup>25</sup> the degree of agreement between these two methods is currently unknown for the muscles crossing the knee joint.

Accuracy of moment arm calculation is contingent on the identification of muscle origin–insertion sites defining the muscle path, as well as application of proper kinematic boundary conditions approximating *in vivo* motion.<sup>2,32,34</sup> Substantial variability exists in identification of muscle origins and insertions, due to the uncertainty in locating anatomical landmarks<sup>8</sup> and estimation of attachment sites as points from irregular areas on the surface of the bones. The importance of kinematics was highlighted by Arnold *et al.*, who observed a strong agreement between measured and predicted moment arms when experimental kinematics were used rather than scaled kinematics.<sup>2</sup> In addition, several studies have reported *in vivo* kinematic variability in natural and implanted knees.<sup>10,22,38</sup> By accounting for such variability while modeling a physiological system, probabilistic methods predict means and bounds of output performances, which can better represent the empirical data.

Therefore, the aims of this study were: (1) to compare flexion–extension moment arms of the major muscles crossing the knee joint obtained by TE and geometric methods; and (2) to quantify the effects of muscle origin–insertion location uncertainty and tibiofemoral kinematic variability on moment arms predicted with the two methods using probabilistic methods. A probabilistic approach represents the input parameters as distributions in order to predict distributions of performance measures, in this case muscle moment arms. In addition, such methods lend insight into parameter interaction effects and quantify the sensitivity of a performance measure to input variables. While previous studies have explained that the variation in observed moment arms may partially be due to uncertainty in muscle origin–insertion locations<sup>5,32</sup> or kinematic differences,<sup>2</sup> the current study uniquely applies probabilistic FE modeling to systematically quantify the effects of such variability on muscle moment arms and identify the important input parameters.

## METHODS

### *Deterministic Model*

An FE-based musculoskeletal model of the right lower extremity was developed (Fig. 1, Table 1) using images from a healthy normal subject. The model comprised of bone geometry: pelvis, femur, patella, tibia, fibula, foot; four flexor muscles: semimembranosus (SMEM), semitendinosus (STEN), and biceps femoris

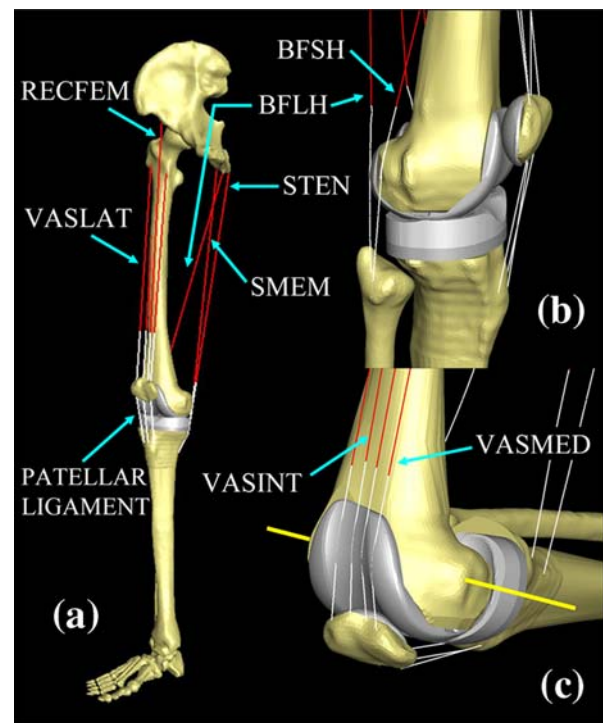


**FIGURE 1.** Explicit finite element (FE) model of a total knee arthroplasty (TKA) implanted right lower extremity with eight musculotendon units and the patellar ligament. The patellar ligament was represented as a series of three stiff connector elements (a). Tendons were modeled using a series of inextensible truss elements able to wrap around bone and implant surfaces (b and c), while muscle fibers were modeled using single connector elements. A representative instantaneous screw axis to calculate moment arm using the geometric origin–insertion method is shown (c).

long and short heads (BFLH and BFSH); four extensor muscles: rectus femoris (RECFEM), vastus lateralis (VASLAT), vastus medialis (VASMED), and vastus intermedius (VASINT); and the patellar ligament. Similar to Buford *et al.*,<sup>6</sup> the combination of the patella

**TABLE 1.** Skeletal dimensions of the lower extremity hemipelvic model.

	Model (mm)
Maximum inferior–superior dimension of pelvis	201.8
Medial–lateral dimension between ASIS and midline	124.4
Maximum anterior–posterior dimension of pelvis	144.1
Inferior–superior dimension from greater trochanter to lateral epicondyle	407.8
Maximum medial–lateral dimension of distal implanted femur	90.7
Maximum anterior–posterior dimension of distal implanted femur	70.4
Maximum medial–lateral dimension of proximal implanted tibia	82.7
Maximum anterior–posterior dimension of proximal tibia	67.6

ligament and RECFEM was effectively used to model the patellar tendon (PATTEN). The bone geometry was extracted using computer tomography (with slice intervals between 1 and 3 mm). Bone geometry at the knee joint was also extracted using MR images ( $512 \times 512$  pixels, T1-weighted, 3D gradient recalled echo sequence with in plane resolution of 0.56 and 1.5 mm slice thickness; echo time 160, repetition time 2.3/1, flip angle  $40^\circ$ ) and spatially aligned to match the whole bones obtained from computer tomography. Muscle origin–insertion locations were estimated from a combination of MR images and data from Delp *et al.*<sup>9</sup> At the knee joint, the locations of flexor muscles insertions were estimated as the centroids of tendon attachments from sagittal and coronal MR images, while insertion locations of the individual extensor muscles were approximated from Delp *et al.*<sup>9</sup> due to the difficulty in isolating them from the MR images. The attachment locations of muscles origins were approximated from Delp *et al.*<sup>9</sup> A semiconstrained, fixed bearing, posterior cruciate-retaining (PCR) total knee arthroplasty (TKA) was included due to the availability of *in vivo* kinematic data. The modeling, developed in ABAQUS™/Explicit (Abaqus, Inc., Providence, RI), was performed with explicit FE analysis for its efficiency, which is especially important when conducting a probabilistic analysis. The bone surfaces, femoral component, and tibial tray were meshed with approximately 2 mm triangular surface elements, while the tibial insert and the patellar button were meshed with 8-noded hexahedral elements. Rigid body analysis was performed with tibio- and patello-femoral contact defined using a previously verified non-linear pressure–overclosure relationship.<sup>14</sup> Tendons were modeled using a series of inextensible truss elements able to wrap around bone and implant surfaces, while muscle fibers were modeled using single connector elements. The patellar ligament was represented as a series of three stiff connector elements (Fig. 1). Contact was included between tendon and bone-implant construct to allow wrapping.

*In vivo* single plane fluoroscopic kinematic data averaged from six patients with the same PCR implants were applied to the lower extremity FE model at the knee joint.<sup>28</sup> The position and orientation of the femoral component with respect to the tibial tray was extracted during weight-bearing knee flexion from  $0^\circ$  to  $90^\circ$ . The geometric centers of the implant components were used as the reference frames in the kinematic study.<sup>28</sup> With the pelvis and the implanted femur fixed at full extension, flexion (from  $0^\circ$  to  $90^\circ$ ), anterior–posterior (AP) translation, and internal–external (IE) rotation were applied to the implanted tibia with respect to the femoral component. The tibia was unconstrained in medial–lateral (ML) and varus–valgus degrees of freedom. A compressive load of 750 N was applied to maintain tibiofemoral contact, while patellofemoral contact during the range of flexion was preserved by applying a nominal load to the extensor muscles. The model output was musculotendon lengths ( $l^m$ ) for each muscle throughout the range of flexion.

Moment arms were calculated for the muscles using the two common methods. The TE method, based on the principle of virtual work, estimated moment arm for a musculotendon unit as the change in length with respect to change in knee flexion angle ( $d(l^m)/d\theta$ ).<sup>1</sup> A geometric method was also used to predict moment arms. From the FE model, the ISA<sup>4,36</sup> was calculated for the range of flexion angles. Moment arms were calculated by determining the orthogonal distance between the ISA and the muscle lines-of-action.<sup>4,32</sup>

### Probabilistic Modeling

Probabilistic methods were implemented to evaluate the impact of uncertainty in muscle origin–insertion location and kinematics on calculated moment arms (Fig. 2). Eight normally distributed input parameters were included in this study: AP translation

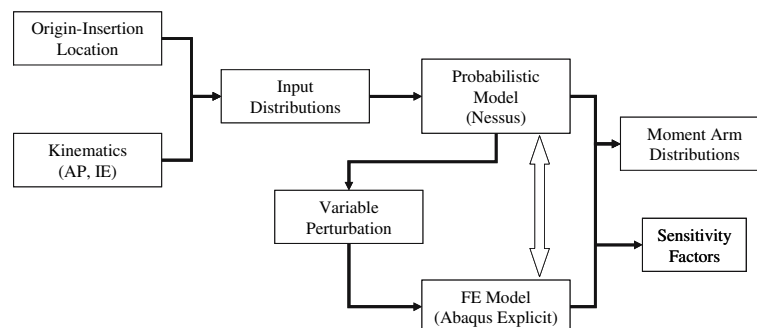


**FIGURE 2.** Schematic of the probabilistic analysis software Nessus (SwRI, San Antonio, TX) linked with the finite element (FE) package Abaqus (Abaqus, Inc., Providence, RI) by custom scripting. Using the eight input parameters represented as normal distributions, Nessus performed the variable perturbations. The modified FE model was run using Abaqus/Explicit and the resulting moment arm predictions along with the sensitivity factors were obtained over the entire flexion cycle.

(AP\_Trans), IE rotation (IE\_Rot), and the AP, ML and inferior–superior (IS) spatial coordinates of the muscle origin (Origin\_AP, Origin\_ML, Origin\_IS) and insertion (Insertion\_AP, Insertion\_ML, Insertion\_IS). Mean values for muscle origin and insertion sites were estimated from Delp *et al.*<sup>9</sup> and MR images, respectively; a single standard deviation of 5 mm, comparable to the range of landmark location errors reported in literature,<sup>21,34</sup> was assumed for all the coordinates of the muscle origin–insertion parameters. For AP translation and IE rotation, mean values and variable standard deviations (up to 1.6 mm and 3.0°) as a function of flexion were obtained from fluoroscopy data.<sup>28</sup> The Advanced Mean Value (AMV) method, applied using Nessus® (SwRI, San Antonio, TX), utilizes optimization to efficiently determine the combination of parameter values that corresponds to performance at a specific probability level.<sup>11,13,37</sup> For well-behaved monotonic systems, AMV exhibits excellent agreement with Monte Carlo simulation with substantial computational savings.<sup>11,24</sup>

The model-predicted envelopes of moment arm results from the geometric and TE methods for the muscles crossing the knee joint. The envelopes were represented as 1–99% confidence intervals (CI) corresponding to  $\pm 3$  standard deviations. Sensitivity factors for the moment arms were also determined. The sensitivity factors are relative measures of how much a probabilistic output metric, i.e., moment arm, was affected by each input parameter. In this study, the sensitivity factors reported are a relative measure computed in the implementation of the AMV method.<sup>11,37</sup> The sensitivity factors can vary at different locations of the flexion cycle; to provide a straightforward ranking of the input parameters, absolute average of the sensitivity was calculated for the entire flexion cycle.

## RESULTS

Peak-predicted moment arm values calculated from the deterministic model ranged from 40.1 to 87.5 mm for the various muscles and the patellar tendon (Figs. 3 and 5a, Table 2). In general, moment arm results obtained from the two methods were similar for the flexor muscles, while more substantial differences between the methods were observed for the extensor muscles and the patellar tendon (Figs. 3 and 5a, Table 2). The average absolute difference over the cycle between the deterministic moment arm values from the two methods was 1.4 mm for the flexors, 18.5 mm for the extensor muscles, and 9.4 mm for the patellar tendon. The geometric method tended to produce larger estimates of peak moment arms for the extensor muscles,

with peak moment arms for the geometric method exceeding those for TE by an average of 9.7 mm.

Accounting for uncertainty in joint kinematics and muscle origin–insertion locations resulted in substantial variability in moment arm predictions (Figs. 3 and 5a, Table 2). The maximum predicted 1–99% CIs were 41.3 mm (TE) and 35.8 mm (geometric) for BFLH, representing 72.8% (TE) and 63.1% (geometric) of the deterministic result at that temporal location (Table 2). The geometric method demonstrated smaller predicted envelope sizes as a result of input variability (assigned distribution in input parameters), with average predicted 1–99% CI from all the muscles and the patellar tendon being 17.2 mm, compared to 25.8 mm from the TE method (Table 2). To calculate the 1 and 99% CIs for the nine musculotendon units, the AMV method required 189 iterations at  $\sim 10$  min per iteration.

The absolute averages of the sensitivities provide a relative ranking of the input parameters on predicted moment arms (Figs. 4 and 5b). The impact of each parameter varied between both the muscles and the methods used to estimate moment arms. For the extensor muscles and the patellar tendon, the origin IS and AP locations, along with the AP location of insertion were the important parameters using the TE method; the critical parameter from the geometric method was the AP location of muscle insertion, followed by lesser contributions from other insertion coordinate axes (InsertionML, InsertionIS) and AP translation (Figs. 4a–4d, and 5b). Flexor muscle moment arms using TE were most sensitive to IS and AP locations of muscle origins and insertions, and to a lesser extent, IE rotation (Figs. 4e–4h); from the geometric method, the important sensitivity factors were IS and AP locations of muscle insertion. In general, moment arm predictions from TE were less sensitive to the kinematic variables than the geometric method, and the flexor muscles estimates were more sensitive to the kinematic variables than the extensor muscles.

## DISCUSSION

An FE-based musculoskeletal model of the lower extremity with an implanted TKA was created to compare moment arm results from TE and geometric methods for the major muscles crossing the knee joint. While a TKA-implanted model was used because of available kinematic data, a similar methodology could be used to predict moment arm estimates from a natural knee. The model was kinematically driven in flexion, AP, and IE using data obtained from video fluoroscopy of weight-bearing knee bends, and

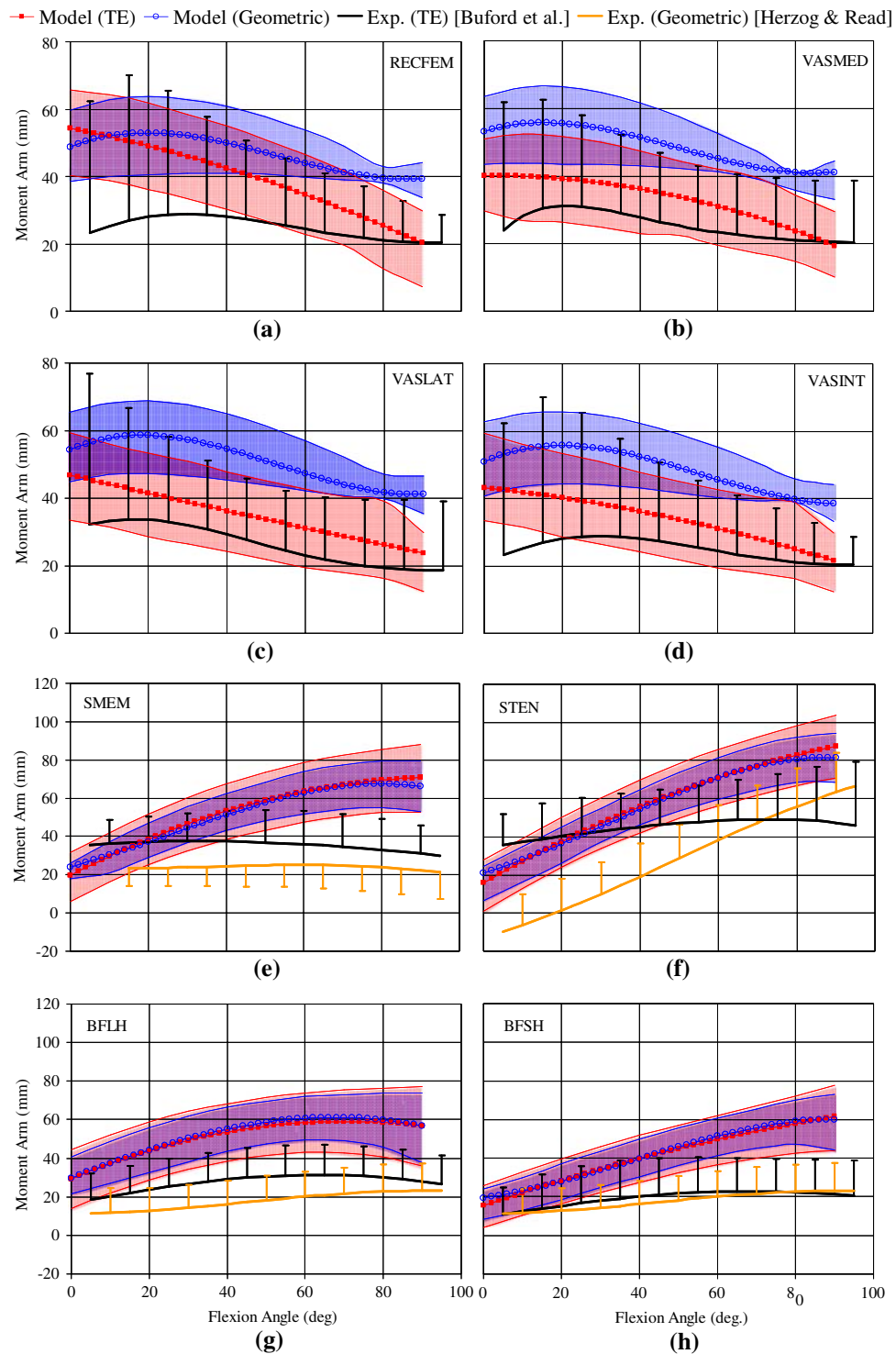


**FIGURE 3.** Predicted moment arms (deterministic and 1–99% confidence intervals) for the eight extensor/flexor muscles as a function of knee flexion. Experimental data for tendon excursion (TE) and geometric methods were obtained from Buford *et al.*<sup>6</sup> and Herzog and Read,<sup>15</sup> respectively. Error bars on the experimental data represent three standard deviations.

compressive load was applied to maintain contact in the tibiofemoral joint. Inextensible truss elements were used as tendons and incorporated contact between the musculotendon units and surrounding bone and

implant geometries. Probabilistic methods were incorporated with the FE model to evaluate the effects of tibiofemoral joint kinematic variability and uncertainty in muscle attachment due to the variability in

**TABLE 2. Deterministic and 1–99% confidence interval (CI) moment arm results along with previously reported experimental data.**

Muscle	Deterministic model			Probabilistic model				Experimental data	
	Peak moment arm (mm)		Average absolute difference (mm)	Average 1–99% CI (mm)		Maximum 1–99% CI (mm)		Average $\pm 3\sigma$ CI (mm)	
	TE	Geometric		TE	Geometric	TE	Geometric	TE <sup>6</sup>	Geometric <sup>15</sup>
RECFEM	54.2	52.9	19.0	24.3	16.5	25.7	23.7	34.5	–
VASMED	40.1	55.8	21.8	22.7	15.7	25.6	23.1	44.5	–
VASLAT	46.8	58.6	18.6	23.3	16.6	25.9	21.7	44.7	–
VASINT	43.1	55.7	14.7	23.3	16.6	25.9	22.1	48.4	–
SMEM	70.8	67.5	1.7	29.7	19.7	35.4	26.7	30.6	23.0
STEN	87.5	81.6	1.5	28.6	20.5	32.7	25.5	43.0	36.5
BFLH	59.1	61.2	1.2	32.1	24.3	41.3	35.8	29.9	25.8
BFSH	61.4	60.1	1.1	25.8	19.9	34.6	28.8	35.7	25.8
PATTEN	54.8	50.1	9.4	22.8	5.3	23.7	6.1	35.8	33.0

Experimental data for tendon excursion (TE) and geometric methods were obtained from Buford *et al.*<sup>6</sup> and Herzog and Read,<sup>15</sup> respectively. Note that Herzog and Read<sup>15</sup> calculated moment arm as distance from tibiofemoral contact point to the line of action of muscle or ligament.

identification of anatomical landmarks and estimation of attachment sites as points from irregular surface areas on predicted muscle moment arms. The efficient AMV method required 189 iterations, a fraction of the number of trials (typically greater than 1000) associated with a Monte Carlo analysis.<sup>11,24</sup> Sensitivity factors were calculated to obtain a relative ranking of the input parameters, and differences in critical parameters between the muscles as well as the methods were highlighted.

Agreement between deterministic moment arm calculations from TE and geometric methods was excellent for the flexor muscles, while differences in trends and magnitudes were observed for the extensor muscles (Fig. 3). One reason for these differences in the extensor muscles moment arms may be the effects of patellofemoral interaction, which has been acknowledged as a potential limitation of the TE method when considering multiple joint interactions.<sup>29</sup> The differences in predicted deterministic moment arms from TE and geometric methods were less for the patellar tendon (Fig. 5a) when compared to an individual extensor muscle (Fig. 3), with average difference being 9.4 mm for PATTEN in comparison to at least 14.7 mm (VASINT) for an extensor muscle (Table 2); this suggests that the consideration of patellar tendon moment arms may be more appropriate than individual extensor muscles.<sup>23,30</sup>

Due to the lack of experimental moment arm data on TKA-implanted lower limbs in the literature, the model predictions were compared to available data from natural knees. Deterministic knee flexion–extension moment arms calculated with the explicit FE model agreed reasonably with the reported experimental data<sup>6,15</sup> (Figs. 3 and 5a), with model predictions for the flexor muscles generally being

greater than the experimental data at higher flexion angles. The average difference over the flexion cycle between predicted deterministic and experimental data for the TE method was 9.3 mm from the extensor muscles (Figs. 3a–3d); while no experimental data were available to compare moment arms predicted from the geometric method for the extensors. For the flexor muscles, comparison of predicted deterministic moment arms with experimental data yielded greater differences, with the maximum average difference over the flexion cycle being 31.4 mm from the geometric method between model-predicted and experimental data<sup>15</sup> for the SMEM muscle (Fig. 3e). Average difference between predicted and experimental data for the geometric method was 1.9 mm for PATTEN (Fig. 5a). Disparity between model-predicted and experimental deterministic values may be due to anthropometric variations, the presence of a TKA in the model, or differing mean kinematics. Differences in moment arm calculation techniques may also account for such disparity; for example, the FE model calculated geometric moment arm as distance from ISA to the line of action of a muscle, compared to distance from the tibiofemoral contact point used by Herzog and Read.<sup>15</sup> Since the location of the ISAs on the femur are farther than the tibiofemoral contact points from a flexor muscle line of action, this explains the consistently greater moment arms predicted by the model using the geometric method (Figs. 3e–3h). The generally greater moment arm predictions from the TE method (Fig. 3) was most likely due to a bowstringing effect;<sup>6,7</sup> in the absence of retinacular restraint, the musculotendon elevates away from the knee center of axis, thus increasing muscle excursion and predicted moment arm.<sup>7</sup>

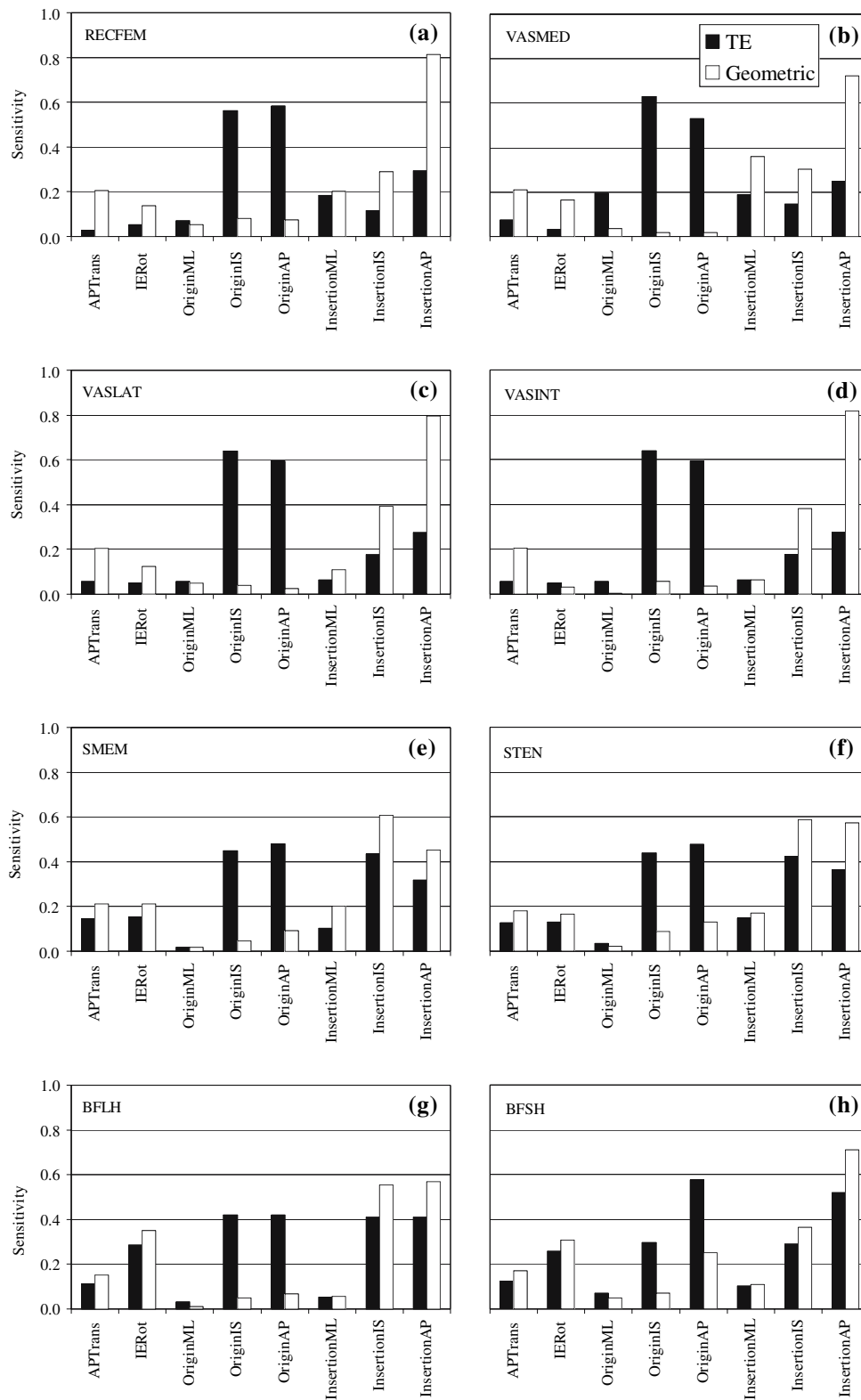


**FIGURE 4.** Sensitivity of predicted muscle moment arms to input parameters. The absolute values of the sensitivities were averaged over the flexion cycle.

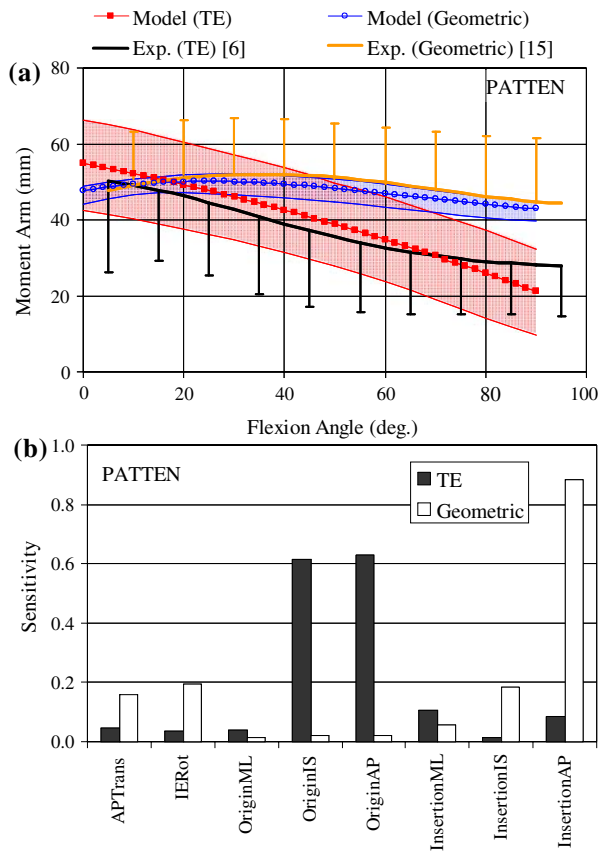


**FIGURE 5.** (a) Predicted moment arms (deterministic and 1–99% confidence intervals) for the patellar tendon as a function of knee flexion. Experimental data for tendon excursion (TE) and geometric methods were obtained from Buford *et al.*<sup>6</sup> and Herzog and Read,<sup>15</sup> respectively. Error bars on the experimental data represent three standard deviations. (b) Sensitivity of predicted patellar tendon moment arms to input parameters. The absolute values of the sensitivities were averaged over the flexion cycle.

The predicted 1–99% moment arm results from the geometric method varied in distribution about the deterministic values with knee flexion (Fig. 3). The extensor muscle CIs were more normally distributed at lower flexion angles and skewed (such that the deterministic values were closer to one extreme) at higher flexion angles. The opposite was true for the flexors, where the CIs were skewed at lower flexion angles and more normally distributed at higher flexion angles. These observed trends in CI distributions were a consequence of tendon contact definition with surrounding surfaces. At flexion angles where a muscle wrapped around the same geometries, the effects of origin–insertion variability on a muscle line of action were diminished, essentially reducing differences in output moment arms from the deterministic values. In contrast, the 1–99% CIs from TE were normally distributed throughout the flexion cycle as TE is estimated independent of muscle line of action.

The substantial variability in moment arm predictions (up to 72.8% from TE and 63.1% from geometric method) has the potential to affect predicted joint moments by also influencing a muscle’s operating range on the force–length curve. The operating range on the force–length curve can be measured by the ratio of the fiber excursion to the optimal fiber length.<sup>16</sup> In order to understand how the distribution of predicted moment arms may impact force–length behavior, ratios of fiber excursions to optimal fiber lengths (obtained from Delp<sup>9</sup>) corresponding to the 1 and 99% CIs from geometric method were averaged throughout the flexion cycle and superimposed on a normalized force–length curve obtained from Zajac<sup>40</sup> (Fig. 6). The average ratio varied from 0.67 (1%) to 0.83 (99%) for RECFEM and 0.40 (1%) to 0.49 (99%) for STEN. These results indicate that the predicted 1–99% distribution of moment arms for a muscle influences its operating range on the force–length curve, thus affecting predicted joint moments.

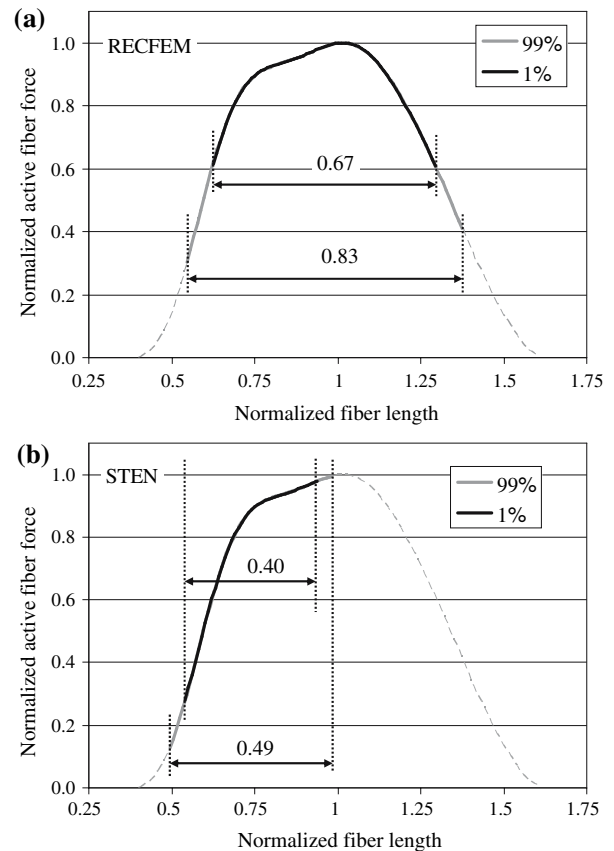


**FIGURE 6.** Ratios of fiber excursions to optimal fiber lengths obtained from 1 and 99% moment arm confidence intervals superimposed on a normalized force–length curve (dashed line) for (a) rectus femoris (RECFEM) and (b) semitendinosus (STEN) muscles.



The sensitivity factors identified the critical and non-critical parameters for the predicted muscle moment arms. The important input parameters from the TE method were the IS and AP locations of muscle origins and insertions (Figs. 4 and 5b). With knee flexion being the dominant joint motion in this study, small changes in AP and IS origin–insertion sites greatly affected the musculotendon excursions of the long muscles in the sagittal plane. In contrast, moment arm predictions using the geometric method were more sensitive to the location of muscle insertion than origin because of the proximity of the insertion sites to the ISA, as observed by Murray *et al.*<sup>26</sup> Contributions of the kinematic parameters to moment arm variability were greater in the geometric method, since TE is less dependent on joint kinematics.<sup>32</sup> Joint translations and out of plane rotations, however, introduce small errors in moment arm calculation using TE,<sup>32</sup> and this was reflected in the kinematic sensitivity factors for the flexor muscles (Figs. 4a–4d); these effects were minimal in the extensors due to the consistent wrapping of the quadriceps muscles over the femoral component resulting in little change in muscle excursion regardless of variability in tibiofemoral kinematics.

In this study, it is important to note that the standard deviations for origin and insertion locations were equal for all coordinate axes and muscles. This decision was made primarily because of the lack of availability of standard deviations for attachment locations for the complete set of muscles. The analysis performed with a constant standard deviation level can provide an important initial assessment of the relative importance of these individual parameters. The origin and insertion sites for the muscles evaluated likely have varying standard deviations that account for muscles originating at large areas of bone and inserting via a tendon to a relatively small area. In addition, variability in attachment site location is also dependent on the coordinate axes, with greater location uncertainty observed along the IS direction of the long bones than along the AP and ML directions.<sup>34</sup> If a complete set of experimentally measured standard deviations for the origin and insertion locations were available, the approach applied here could be similarly implemented to assess the variability in muscle moments arms for the measured data. It is also important to note that there is substantial uncertainty in the isolation of insertion locations of individual extensor muscles from MR images, which serves as a motivation for the current probabilistic study.

A potential limitation of this model was that linear segments were used to represent complex musculotendon architectures. The lines of action of the linear segments may not accurately represent the lines of action of the centroids of muscle fibers and tendons for

all joint angles, and may account for some of the discrepancies between model-predicted and experimental moment arm values. Blemker and Delp created 3D FE models of complex muscle architecture,<sup>3</sup> but these models are computationally expensive and unsuitable for running a large number of iterations required for a probabilistic study. It should also be noted that the deterministic moment arm predictions are based on one lower extremity data set; using a single model provides a direct comparison between the two types of moment arm measurement techniques and lends insight into the differences in the important parameters affecting each measurement technique. The addition of complex muscle architectures or anthropometric uncertainties (from multiple subjects) as inputs to the probabilistic study would most likely increase the CIs of the predicted moment arms. However, there is currently no algorithm for efficient scaling of anthropometric differences.<sup>32</sup> Further, the sensitivities are dependent on the standard deviations associated with each input parameter. If anthropometric parameters are considered, it is not intuitively obvious if a model of a larger individual would be more sensitive to kinematics or a smaller model would be more sensitive to muscle attachment location due to interaction between all the input parameters. Additional work is required to understand the effects of anthropometric differences with uncertainty in muscle attachment and kinematic variability. Also, the pelvis angles were not specified as a function of knee flexion, which may affect musculotendon excursions and moment arm predictions from the TE method. Simultaneous *in vivo* kinematic data for femoro-pelvic and tibio-femoral joints were not available, and the difference in moment arms due to the addition of pelvic rotations is anticipated to be small. While the present study was performed for a TKA-implanted model, a natural knee representation would likely predict similar bands of performance, given the same methods, muscle attachment uncertainty, and substantial variability in kinematics also observed in the natural knee.<sup>22</sup>

In closing, a musculoskeletal model of the lower extremity was developed integrating probabilistic methods with explicit FE analysis to assess the impact of origin–insertion location and joint kinematic variability on moment arm predictions using TE and geometric methods. Agreement between the deterministic moment arms from the two methods was excellent for the flexor muscles. The 1–99% CIs represented up to 72.8% variability of the mean predicted moment arms for the standard deviation levels evaluated. In addition, the sensitivity factors identified the important parameters for each moment arm calculation method, highlighting the importance of muscle origin–insertion locations over kinematic variables at the levels

investigated. The framework developed in this study can be further used to characterize the effects of different TKA designs and implant alignment on muscle moment arms, lending valuable insight into changes in predicted joint moments with TKA implantation.

### ACKNOWLEDGMENT

This research was supported in part by DePuy, a Johnson & Johnson Company.

### REFERENCES

- <sup>1</sup>An, K. N., B. M. Kwak, E. Y. Chao, and B. F. Morrey. Determination of muscle and joint forces: A new technique to solve the indeterminate problem. *J. Biomech. Eng.* 106:364–367, 1984.
- <sup>2</sup>Arnold, A. S., S. Salinas, D. J. Asakawa, and S. L. Delp. Accuracy of muscle moment arms estimated from MRI-based musculoskeletal models of the lower extremity. *Comput. Aided Surg.* 5:108–119, 2000.
- <sup>3</sup>Blemker, S. S., and S. L. Delp. Rectus femoris and vastus intermedius fiber excursions predicted by three-dimensional muscle models. *J. Biomech.* 39:1383–1391, 2006.
- <sup>4</sup>Boyd, S. K., and J. L. Ronsky. Instantaneous moment arm determination of the cat knee. *J. Biomech.* 31:279–283, 1998.
- <sup>5</sup>Brand, R. A., R. D. Crowninshield, C. E. Wittstock, D. R. Pedersen, C. R. Clark, and F. M. van Krieken. A model of lower extremity muscular anatomy. *J. Biomech. Eng.* 104:304–310, 1982.
- <sup>6</sup>Buford, W. L. Jr., F. M. Ivey Jr., J. D. Malone, R. M. Patterson, G. L. Peare, D. K. Nguyen, and A. A. Stewart. Muscle balance at the knee—moment arms for the normal knee and the ACL-minus knee. *IEEE Trans. Rehabil. Eng.* 5:367–379, 1997.
- <sup>7</sup>Burkholder, T. J., and R. L. Lieber. Sarcomere number adaptation after retinaculum transection in adult mice. *J. Exp. Biol.* 201:309–316, 1998.
- <sup>8</sup>della Croce, U., A. Cappozzo, and D. C. Kerrigan. Pelvis and lower limb anatomical landmark calibration precision and its propagation to bone geometry and joint angles. *Med. Biol. Eng. Comput.* 37:155–161, 1999.
- <sup>9</sup>Delp, S. Surgery simulation: A computer-graphics system to analyze and design musculoskeletal reconstructions of the lower limb. PhD thesis, Stanford University, 1990.
- <sup>10</sup>Dennis, D. A., R. D. Komistek, M. R. Mahfouz, B. D. Haas, and J. B. Stiehl. Multicenter determination of in vivo kinematics after total knee arthroplasty. *Clin. Orthop. Relat. Res.* 416:37–57, 2003.
- <sup>11</sup>Easley, S. K., S. Pal, P. R. Tomaszewski, A. J. Petrella, P. J. Rullkoetter, and P. J. Laz. Finite element-based probabilistic analysis tool for orthopaedic applications. *Comput. Methods Programs Biomed.* 85:32–40, 2007.
- <sup>12</sup>Gill, H. S., and J. J. O'Connor. Biarticulating two-dimensional computer model of the human patellofemoral joint. *Clin Biomech.* 11:81–89, 1996.
- <sup>13</sup>Haldar, A., and S. Mahadevan. Probability, Reliability and Statistical Methods in Engineering Design. New York, NY: Wiley & Sons, Inc., 2000.
- <sup>14</sup>Halloran, J. P., S. K. Easley, A. J. Petrella, and P. J. Rullkoetter. Comparison of deformable and elastic foundation finite element simulations for predicting knee replacement mechanics. *J. Biomech. Eng.* 127:813–818, 2005.
- <sup>15</sup>Herzog, W., and L. J. Read. Lines of action and moment arms of the major force-carrying structures crossing the human knee joint. *J. Anatomy* 182:213–230, 1993.
- <sup>16</sup>Hoy, M. G., F. E. Zajac, and M. E. Gordon. A musculoskeletal model of the human lower extremity: the effect of muscle, tendon, and moment arm on the moment–angle relationship of musculotendon actuators at the hip, knee, and ankle. *J. Biomech.* 23:157–169, 1990.
- <sup>17</sup>Hughes, R. E., G. Niebur, J. Liu, and K.-N. An. Comparison of two methods for computing abduction moment arms of the rotator cuff. *J. Biomech.* 31:157–160, 1998.
- <sup>18</sup>Imran, A., R. A. Huss, H. Holstein, and J. J. O'Connor. The variation in the orientations and moment arms of the knee extensor and flexor muscle tendons with increasing muscle force: a mathematical analysis. *Proc. Inst. Mech. Eng. [H]*. 214:277–286, 2000.
- <sup>19</sup>Karlsson, D., and B. Peterson. Towards a model for force predictions in the human shoulder. *J. Biomech.* 25:189–199, 1992.
- <sup>20</sup>Kellis, E., and V. Baltzopoulos. In vivo determination of the patella tendon and hamstrings moment arms in adult males using videofluoroscopy during submaximal knee extension and flexion. *Clin. Biomech.* 14:118–124, 1999.
- <sup>21</sup>Kepple, T. M., A. S. Arnold, S. J. Stanhope, and K. L. Siegel. Assessment of a method to estimate muscle attachments from surface landmarks: a 3D computer graphics approach. *J. Biomech.* 27:365–371, 1994.
- <sup>22</sup>Komistek, R. D., D. A. Dennis, and M. Mahfouz. In vivo fluoroscopic analysis of the normal human knee. *Clin. Orthop. Relat. Res.* 410:69–81, 2003.
- <sup>23</sup>Krevolin, J. L., M. G. Pandy, and J. C. Pearce. Moment arm of the patellar tendon in the human knee. *J. Biomech.* 37:785–788, 2004.
- <sup>24</sup>Laz, P. J., S. Pal, J. P. Halloran, A. J. Petrella, and P. J. Rullkoetter. Probabilistic finite element prediction of knee wear simulator mechanics. *J. Biomech.* 39:2303–2310, 2006.
- <sup>25</sup>Maganaris, C. N. Imaging-based estimates of moment arm length in intact human muscle-tendons. *Eur. J. Appl. Physiol.* 91:130–139, 2004.
- <sup>26</sup>Murray, W. M., T. S. Buchanan, and S. L. Delp. Scaling of peak moment arms of elbow muscles with upper extremity bone dimensions. *J. Biomech.* 35:19–26, 2002.
- <sup>27</sup>Murray, W. M., S. L. Delp, and T. S. Buchanan. Variation of muscle moment arms with elbow and forearm position. *J. Biomech.* 28:513–525, 1995.
- <sup>28</sup>Pal, S., C. Hammill, P. Rullkoetter, M. Mahfouz, and R. D. Komistek. In vivo determination of tibiofemoral contact for subjects having PS and PCR TKA. *Trans. ORS.* 29:1380, 2004.
- <sup>29</sup>Pandy, M. G. Moment arm of a muscle force. In: Exercise and Sport Sciences Reviews, edited by J. O. Holloszy. Philadelphia, PA: Lippincott Williams & Wilkins, 1999, pp. 79–118.
- <sup>30</sup>Smidt, G. L. Biomechanical analysis of knee flexion and extension. *J. Biomech.* 6:79–92, 1973.
- <sup>31</sup>Spoor, C. W., J. L. van Leeuwen, W. J. van der Meulen, and A. Huson. Active force–length relationship of human lower-leg muscles estimated from morphological data: a comparison of geometric muscle models. *Eur. J. Morphol.* 29:137–160, 1991.

- <sup>32</sup>Tsaopoulos, D. E., V. Baltzopoulos, and C. N. Maganaris. Human patellar tendon moment arm length: measurement considerations and clinical implications for joint loading assessment. *Clin. Biomech.* 21:657–667, 2006.
- <sup>33</sup>van der Helm, F. C. T. A finite element musculoskeletal model of the shoulder mechanism. *J. Biomech.* 27:551–569, 1994.
- <sup>34</sup>White, S. C., H. J. Yack, and D. A. Winter. A three-dimensional musculoskeletal model for gait analysis. Anatomical variability estimates. *J. Biomech.* 22:885–893, 1989.
- <sup>35</sup>Wilson, D. L., Q. Zhu, J. L. Duerk, J. M. Mansour, K. Kilgore, and P. E. Crago. Estimation of tendon moment arms from three-dimensional magnetic resonance images. *Ann. Biomed. Eng.* 27:247–256, 1999.
- <sup>36</sup>Woltring, H. J., K. Long, P. J. Osterbauer, and A. W. Fuhr. Instantaneous helical axis estimation from 3-D video data in neck kinematics for whiplash diagnostics. *J. Biomech.* 27:1415–1432, 1994.
- <sup>37</sup>Wu, Y. T., H. R. Millwater, and T. A. Cruse. Advanced probabilistic structural-analysis method for implicit performance functions. *Aiaa J.* 28:1663–1669, 1990.
- <sup>38</sup>Yoshiya, S., N. Matsui, R. D. Komistek, D. A. Dennis, M. Mahfouz, and M. Kurosaka. In vivo kinematic comparison of posterior cruciate-retaining and posterior stabilized total knee arthroplasties under passive and weight-bearing conditions. *J. Arthroplasty* 20:777–783, 2005.
- <sup>39</sup>Yuen, T. J., and M. S. Orendurff. A comparison of gastrocnemius muscle-tendon unit length during gait using anatomic, cadaveric and MRI models. *Gait Posture.* 23:112–117, 2006.
- <sup>40</sup>Zajac, F. E. Muscle and tendon: properties, models, scaling, and application to biomechanics and motor control. *Crit. Rev. Biomed. Eng.* 17:359–411, 1989.